Thermal mixing between spin systems in Al_2O_3 by a resonant rf electric field

Hiroshi Hatanaka
Department of Physics, Faculty of Education, Kanazawa University, Kanazawa 920 Japan
(Received 20 December 1988)

Spin thermal mixing due to the irradiation of an rf electric field has been observed, for the first time, between a two-level system with $\Delta m = \pm 2$ and a dipolar system of ^{27}Al nuclei in Al_2O_3. The thermal mixing is accomplished in a time much shorter than the spin-lattice relaxation time by applying strong rf electric field with amplitude of about 22 kV/cm at room temperature. Experimental results are sufficiently interpreted by the theory developed by assuming a concept of spin temperature in the rotating frame. A technique of double-quantum adiabatic demagnetization in the rotating frame is used in the experiments.

I. INTRODUCTION

It has been shown in solid-state nuclear magnetic resonance (NMR) that behaviors of spin systems under irradiations of a strong rf magnetic field can be described in terms of spin temperature in the rotating frame.[1] The behaviors involve adiabatic demagnetization,[2] double resonance,[3] and several types of thermal mixing[4] in the rotating frame. Provotorov proposed a saturation theory,[5] where the saturation of nuclear magnetic resonance is understood as a result of thermal mixing between Zeeman and dipolar systems in the rotating frame. It is pointed out[6] that even though the intensity of an applied rf magnetic field H_1 is smaller than the local field the concept of spin temperature is valid in the rotating frame, as long as H_1 satisfies a condition $\gamma^2 H_1^2 T_1 T_2' \gg 1$, where γ, T_1, and T_2' are a gyromagnetic ratio of spins, spin-lattice relaxation time, and decay time of transverse magnetization, respectively.

The concept of spin temperature has been applied to double-quantum (DQ) NMR ($\Delta m = \pm 2$).[7] The DQ coherence is usually excited with an rf magnetic field via an intermediate state[8] or by two-step excitations.[9]

The DQ transition can also be excited by an rf electric field[10,11] or an ultrasonic wave[12] through a dynamic electric quadrupole (EQ) interaction. In contrast to the excitation by the rf magnetic field, it is usually difficult to strongly excite the transition by this type of method (referred to as EQ excitation) because the excitation efficiency is very low. Most experimental studies made so far by using EQ excitation were confined to steady-state saturations under the influence of spin-lattice relaxation.

The present paper reports on the first observation of the thermal mixing produced by the EQ excitation using an rf electric field. We have realized the strong EQ excitation for the DQ transition, and observed the thermal mixing between the two-level system with $\Delta m = \pm 2$ (the DQ Zeeman system) and the dipolar system. This type of thermal mixing occurs at slightly off resonance but not at exact resonance. By strong excitation we mean that it satisfies the condition.

$$\omega_p^2 T_1 T_2 \gg 1 , \tag{1}$$

where ω_p shows a strength of the EQ excitation corresponding to γH_1, and T_2 is the decay time of the DQ coherence or the decay time of the DQ free decay.[8,13]

The experiment was performed on ^{27}Al nuclei in Al_2O_3 at room temperature. In order to overcome effects of indirect EQ saturation[14] and satisfy the strong excitation condition (1), the rf electric field with intensity of about 22 kV/cm was used. By this strong rf electric field, the thermal mixing was completely accomplished in a time much shorter than $T_1 \simeq 0.5$ s. Therefore, influences of the spin-lattice relaxation on the thermal mixing can be neglected. Two types of the experiments were performed. In one of them the system is prepared to have a low dipolar temperature by using DQ adiabatic demagnetization in the rotating frame (ADRF).[15]

We develop a theory describing the phenomena of the thermal mixing caused by the rf electric field, which is analogous to the Provotorov's saturation theory. Though the rf electric field may also have oscillatory effects on the dipolar interaction via the induced lattice vibrations, the effects on the dipolar interaction are neglected and a dipolar Hamiltonian which has been used in NMR studies on the same spin system[13] is used in the development of the theory. The excellent agreement between the experiments and the theory shows that the concept of spin temperature in the rotating frame is valid when the strong rf electric field is used for the saturation of the DQ transition.

II. EXPERIMENTAL PROCEDURE

A single crystal of Al_2O_3 ($15 \times 10 \times 2$ mm^3) whose 15×10 mm^2 crystal faces are parallel to the c axis has been used. Silver electrodes with thickness of about 15 μm are deposited on these faces to apply the strong rf electric field perpendicular to the c axis. The rf electric field with an amplitude of 10–30 kV/cm (at about 25.6 MHz) is applied for the experiments of the thermal mixing and other relevant experiments. To avoid electric discharge along the crystal faces due to the strong rf electric field, the sample is covered with epoxy (supplied by Murata Mfg. Co., Ltd.). It was confirmed that a DC voltage of 6 kV could be applied for a long time. In order

to apply such a strong rf electric field, no condenser (other than the sample whose capacitance is about 8 pF) was used in the LC resonance circuit which is tuned to the frequency ($\sim$25.6 MHz) of the rf power. The tuning was adjusted by changing the length of the coil of the resonance circuit.

The sample is subjected to a static magnetic field H_0 along the c axis. The Al nuclei are also subjected to a weak and static electric-quadrupole interaction which is axially symmetric around the c axis. Therefore, the energy-level spacing is unequal and no level mixing exists. The energy levels are schematically shown in Fig. 1, and denoted by numbers from 0 to 5 for convenience. The rf electric field excites the transition between levels 1 and 3. The rf electric field may produce a displacement current in the sample. But its effect for the excitation of resonances can be neglected because the level mixing due to the misalignment of the crystal with respect to H_0 is very small. Notations ω_1 and ω_2 are transition frequencies between levels 1 and 2, and 2 and 3, respectively. The magnetic field H_0 is such that $\omega_1=2\pi\times 13$ MHz and $\omega_2=2\pi\times 12.64$ MHz.

Two types of experiments have been carried out. In the first one (I) the rf electric field is applied to the spin system which is in thermal equilibrium at lattice temperature. In the frame rotating around the z axis ($\|H_0$) at the frequency of the rf electric field, the initial spin temperature (absolute value) of the DQ Zeeman system ($1\leftrightarrow 3$) is very small compared with that of the dipolar system. In the second one (II), the DQ ADRF is performed before the application of the rf electric field. Therefore, the spin temperature of the dipolar system is very low and that of the DQ Zeeman system is very high. Trace A in Fig. 2 indicates the procedure of the DQ ADRF, which consists of a DQ 90° pulse[8] followed by DQ spin locking[15,16] and complete demagnetization. The frequency of the DQ pulses is $\frac{1}{2}(\omega_1+\omega_2)$, and the phase of the second pulse is shifted by 45° from the first one. Trace B in Fig. 2 shows the rf electric-field pulse with duration t and frequency

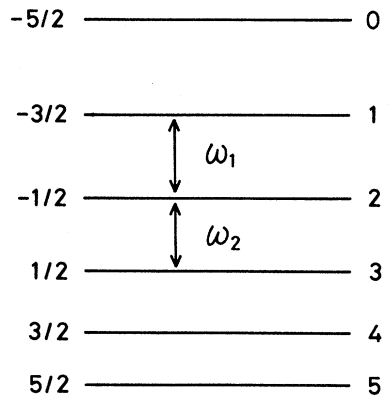

FIG. 1. Energy-level diagram of ^{27}Al nuclei in Al_2O_3. No level mixing exists since H_0 is applied along the principal axis of the static and axially symmetric efg tensor. ω_1 and ω_2 are the transition frequencies between levels 1 and 2 ($2\pi\times 13$ MHz), and 2 and 3 ($2\pi\times 12.64$ MHz), respectively.

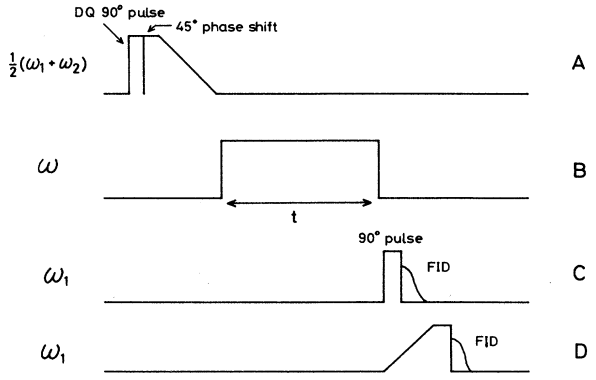

FIG. 2. Operations for two types of experiments of the thermal mixing. In experiment I, the rf electric-field pulse at frequency $\omega\sim\omega_1+\omega_2$ shown by trace B is applied to the spin system in thermal equilibrium at lattice temperature, where the initial absolute value of temperature of the DQ Zeeman system is small in the rotating frame. In experiment, II, the operation of DQ ADRF shown by trace A is applied before the application of the rf electric field in order to initially have the dipolar system at low temperature and the DQ Zeeman system at high temperature. Traces C and D show the pulses for observing the behaviors of w_{13} and the dipolar order, respectively. The latter is the AMRF pulse.

$\omega\simeq\omega_1+\omega_2$. For the present experiment of thermal mixing the rf electric field whose amplitude E_0 is 22.3 kV/cm is used, for which $\omega_p{}^2T_1T_2\simeq 80$. The spin-lattice relaxation time T_1 is about 0.5 s for the sample containing about 0.01% Cr^{3+} ions at room temperature, and T_2 for the transition $1\leftrightarrow 3$ is 38 μs.[13]

The thermal mixing is detected with an aid of the pulse shown by trace C or D in Fig. 2. A 90° pulse in trace C (denoted by the pulse C) is used to observe the free-induction decay (FID) at ω_1. Since $\omega_1-\omega_2\ll\omega_1$, the population difference w_{12} of the levels 1 and 2 is almost one-half the population difference w_{13} of the levels 1 and 3, where w_{ij} is defined by $\rho_{jj}-\rho_{ii}$. Therefore, the change of w_{13} or that of the Zeeman temperature of the system $1\leftrightarrow 3$, which is due to the thermal mixing, can be detected from the amplitude of the FID signal.

Trace D illustrates an operation of the adiabatic magnetization in the rotating frame (AMRF),[17] by which the dipolar order is measured. An rf magnetic field resonant to the transition $1\leftrightarrow 2$ is applied and its amplitude is slowly increased. The final amplitude is much larger than the local field, and then, suddenly turned off. From the initial amplitude of the FID signal at ω_1 after the pulse (denoted by the pulse D), we can measure the degree of the dipolar order or the dipolar temperature, and therefore the effect of thermal mixing.

The initial amplitudes of the FID signals measured by the pulses C and D are denoted by S_1 and S_2, respectively. S_1 and S_2 are measured in units of S_0, which is the initial amplitude of the FID signal observed for the transition $1\leftrightarrow 2$ by applying a 90° pulse to the spin system in thermal equilibrium at lattice temperature.

III. EXPERIMENTAL RESULTS AND DISCUSSIONS

Preliminary experiments were carried out at exact resonance ($\omega=\omega_1+\omega_2$). The rf electric field with amplitude E_0 (10–30 kV/cm) was applied to the sample at lattice temperature. It was observed that the time evolution of population difference w_{13} can be expressed by an exponential function with a saturation rate K_0, which is proportional to E_0^2 as

$$K_0=CE_0^2 , \tag{2}$$

where $C=0.40\pm0.03$ cm^2/(kV^2 s). This shows the saturation of the transition $1\leftrightarrow3$. The thermal mixing did not take place as described later. The value of C can be calculated from Eqs. (A11) and (A15) in the Appendix by using elements of a tensor R determined from the Stark effect of NMR signals in Al_2O_3.[18] The calculated value 0.397 cm^2/(kV^2 s) is in good agreement with the experimental value. Kushida and Silver[10] observed a dependence of K_0 similar to Eq. (2) with a weak rf electric field at 4.2 K. The value of C estimated from their experiment is about seven times as large as the theoretical value. The discrepancy was considered[14] to be due to the indirect excitation via lattice defects. The good agreement of the observed and theoretical values of C in the present study indicates that the rf electric field directly excites the Al spins over the sample.

The dipolar signal was too small to be detected. The fact that the temperature of the dipolar system does not change at exact resonance was confirmed from experiment II.

The thermal mixing was observed when the slightly off resonant rf electric field was applied. Figure 3 shows the time evolutions of $2S_1$ or those of w_{13} observed in experiment I for positive frequency offsets $2\delta=\omega-(\omega_1+\omega_2)$. Solid lines in the figure, and those in Figs. 4–7, are theoretical. Similar experimental results were obtained for $\delta<0$. In both cases, w_{13} decreases exponentially with time t, and reaches a steady-state value. The decay rate of w_{13} decreases and the steady-state value increases as $|2\delta|$ increases. It is noted that the steady-state values are achieved in a time much shorter than the spin-lattice relaxation time T_1.

Figure 4 shows the time evolutions of the dipolar order (S_2) which were observed for $\delta<0$ by using the pulse D. We can see that the dipolar order grows exponentially and finally reaches a steady-state value. In the case of $\delta>0$, similar curves were observed with negative values of S_2, which show the time evolutions of the dipolar order at negative temperatures.

These behaviors of w_{13} and the dipolar order indicate the thermal mixings due to the rf electric field. The qualitative illustration of the phenomena in terms of the spin temperature is as follows.[4] In the case of $\delta<0$, the spacing between the energy levels 1 and 3 is -2δ in the rotating frame. Therefore, the initial spin temperature of the DQ Zeeman system is much lower than the lattice temperature since $-2\delta\ll\omega_1+\omega_2$. The dipolar system is initially at lattice temperature. If -2δ is comparable to γH_L, where H_L is the local field, the irradiation of the rf electric field causes the thermal contact between the DQ Zeeman system and the dipolar system through the induced dynamic electric quadrupole interaction. The heat flows from the dipolar system to the DQ Zeeman system until common temperature is established in the systems. As a result, w_{13} decreases and the dipolar order increases.

When $\delta>0$, the DQ Zeeman system is initially at negative temperature in the rotating frame, that is, the spin population of the upper level is larger than that of the lower one. (The energy of level 3 is higher than that of level 1 in this rotating frame.) The absolute value of the temperature is very small. Therefore, similar thermal mixings occur at negative temperatures.

Open circles in Fig. 5 show a dependence of the dipolar temperature on the frequency ω which was observed at $t=20$ ms. The behavior is just expected from the above argument. A frequency dependence of w_{13} was also ob-

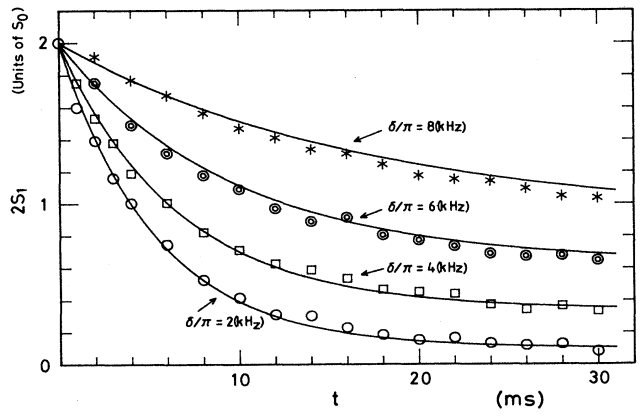

FIG. 3. Time evolutions of the thermal mixing observed on w_{13} by experiment I. w_{13} decreases exponentially and reaches a steady-state value in a time much shorter than $T_1\simeq0.5$ s. Solid lines are the theoretical curves describing Eq. (3a) with $w_{13}(0)=2$ and $G(0)=0$ for the corresponding values of δ.

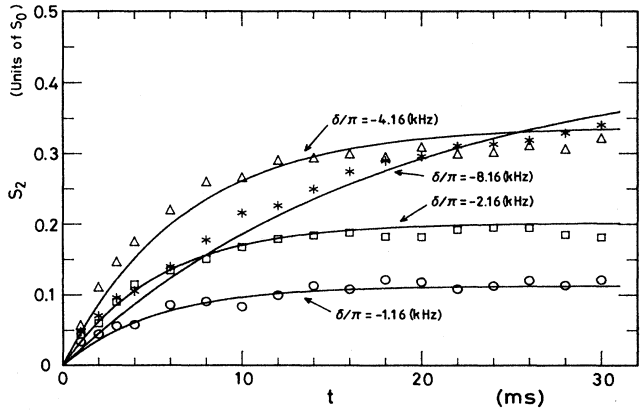

FIG. 4. Time evolutions of the thermal mixing observed on the dipolar order by experiment I. The dipolar order grows exponentially. The observed dipolar signals S_2 were smaller than the theoretical values of $G(t)$ calculated from Eq. (3b) by putting $w_{13}(0)=2$ and $G(0)=0$. The solid lines are the theoretical curves of $AG(t)$ plotted with $A=0.44$, where it is assumed that the operation of AMRF was incomplete.

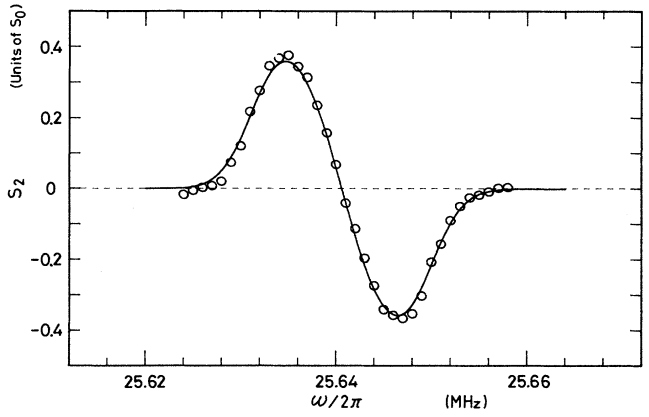

FIG. 5. Dependence of the dipolar order on the frequency ω observed at $t=20$ ms (open circles). The experimental condition is the same as that in Fig. 4. When $\omega>2\pi\times25.64$ MHz ($\delta>0$) negative temperature is established in the dipolar system by the thermal contact with the DQ Zeeman system at negative temperature in the rotating frame. Solid line is theoretical.

served, which presented a conventional saturation curve (not shown in the figure). The linewidth of the transition $1\leftrightarrow3$ estimated from the curve in Fig. 5 or the saturation curve of w_{13} is smaller than those obtained by using a weak electric field[10] and an ultrasonic wave.[19] The discrepancy is also considered to be due to the effect of the lattice defects mentioned earlier, namely, the Al nuclei near the lattice defects which contribute to the indirect saturations are subjected to large inhomogeneities of the internal electric-field gradients, and therefore, have the large linewidth.

In experiment II, the DQ Zeeman system is prepared

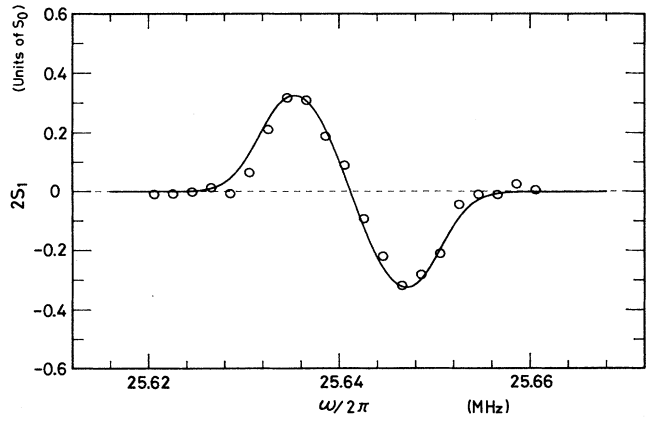

FIG. 6. Frequency dependence of w_{13} observed at $t=20$ ms by experiment II (open circles). The negative population difference ($2S_1<0$) observed at $\omega>2\pi\times25.64$ MHz is due to the fact that the energy of level 3 becomes higher than that of level 1 in the rotating frame. The experimental values were smaller than the theoretical values of w_{13} calculated from Eq. (3a) with $G(0)=2$ and $w_{13}(0)=0$. The solid line is plotted with $G(0)=2B$ and $B=0.40$ under the assumption that the operation of DQ ADRF was incomplete.

at infinite temperature and the dipolar system at very low temperature. Therefore, the heat flows from the DQ Zeeman system to the dipolar system, and, as a result, the population difference increases as the dipolar order decreases in the rotating frame. Open circles in Figs. 6 and 7 show frequency dependences of w_{13} and the dipolar order observed at $t=20$ ms by experiment II, respectively. These curves indicate that w_{13} is created by decreasing the dipolar order. When $\delta>0$, that is, $\omega>2\pi\times25.64$ MHz, w_{13} becomes negative. The negative population difference is also due to the fact that the energy of level 3 becomes higher than that of level 1 in the rotating frame. At $\delta=0$, w_{13} and the dipolar order are unchanged. This indicates that the thermal mixing does not occur at exact resonance.

We developed a theory of the thermal mixing due to the rf electric field. This is similar to that of Provotorov. The dipolar system is characterized by a truncated dipolar Hamiltonian $\mathcal{H}_d^*$ defined in Ref. 13 which has so far been used in NMR studies on the same spin system.[20,21] From the experimental study of DQ free decay[13] it can be assumed that the free decay in the transition $1\leftrightarrow3$ is of a Gaussian shape with $T_2=38$ μs. Effects of the spin-lattice relaxation are neglected because of the rapid thermal mixing. The outline of the theory is shown in the Appendix. We derived a set of equations for the thermal mixing [Eqs. (A14)], which can be solved for the time dependent temperatures of the DQ Zeeman system and the dipolar system. From the solutions, we obtain expressions

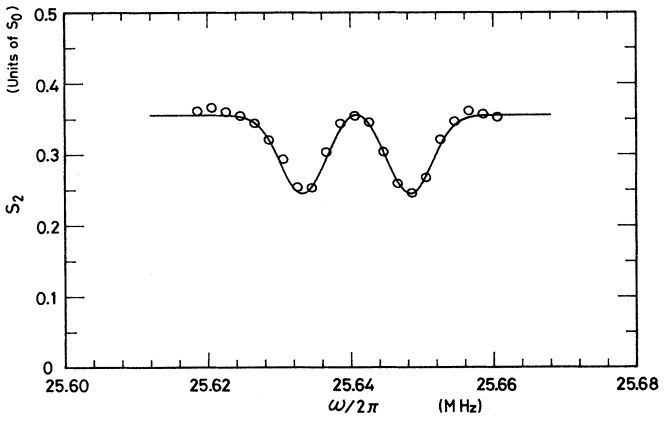

FIG. 7. Frequency dependence of the dipolar order observed under the same experimental condition as that in Fig. 6. Comparing the curve shown by open circles with that in Fig. 6, we can see that the decrease of the dipolar order produces the population difference in the DQ Zeeman system. We also recognize that the thermal mixing does not occur at exact resonance ($\omega=2\pi\times25.64$ MHz). In this experiment, both the operations of AMRF and DQ ADRF are used. Solid line is the theoretical curve plotted based on Eq. (3b) with $A=0.44$ and $B=0.40$. The good agreement between the experimental and the theoretical curves supports the assumptions that the operations of AMRF and DQ ADRF were incomplete.

$$w_{13}(t)=D[Dw_{13}(0)+\delta G(0)]\{\exp[-K(1+\delta^2/D^2)t]-1\}/(\delta^2+D^2)+w_{13}(0)\ , \tag{3a}$$

$$G(t)=\delta[\delta G(0)+Dw_{13}(0)]\{\exp[-K(1+\delta^2/D^2)t]-1\}/(\delta^2+D^2)+G(0)\ , \tag{3b}$$

where

$$K=K_0\exp(-2\delta^2T_2^2)\ ,$$
$$D^2=\mathrm{Tr}(\mathcal{H}_d^{*2})/[2N(2I+1)^{N-1}]\ . \tag{4}$$

$G(t)$ is defined by Eq. (A17), which indicates a degree of the dipolar order, and N is the number of the Al nuclei. The value of D^2 is evaluated to be 775.7 kHz^2 with the value of the geometric factor in $\mathcal{H}_d^*$ which was determined in a previous study.[13]

We represent w_{13} and G in units of w_0 which is the amount of w_{12} in thermal equilibrium at lattice temperature. As shown in the Appendix, such amounts of w_{13} and G are equal to the magnitudes of $2S_1$ and S_2 measured in units of S_0, respectively. Therefore, Eqs. (3) can be compared quantitatively with the experimental results.

Solid lines in Fig. 3 describe calculated values from Eq. (3a) with $w_{13}(0)=2$ for the corresponding amounts of δ, where an approximation $G(0)=0$ is used considering that $G(0)\ll w_{13}(0)$. The experimental curves are well in agreement with the theoretical ones. The similar agreements were also obtained for $\delta<0$.

Equation (3b) should present theoretical curves which coincide with the experimental results in Fig. 4 by putting $w_{13}(0)=2$ and $G(0)=0$. However, the theoretical curves were not in agreement with the experimental ones. The theoretical values were larger than the corresponding experimental values. It is not reasonable to attribute the discrepancies to thermal contacts with the lattice and other systems during the irradiation of the rf electric field, because the good agreements between the experiments and the theory are obtained for w_{13} as shown in Fig. 3. Assuming that the operation of AMRF was incomplete, we plot values $AG(t)$ with a fitting factor A. Solid lines in Figs. 4 and 5 are the theoretical curves plotted with $A=0.44$. In Fig. 5, the values $AG(t)$ at $t=20$ ms are plotted as a function of ω. Agreements between the experimental and the theoretical results are very well though A is smaller than unity. We can conclude from these excellent agreements in Figs. 3, 4, and 5 that the concept of spin temperature in the rotating frame is valid under the irradiation of the strong rf electric field, and the dipolar system represented by the Hamiltonian $\mathcal{H}_d^*$ plays the role of the reservoir.

Solid lines in Figs. 6 and 7 are the theoretical curves of $w_{13}(t)$ and $AG(t)$ at $t=20$ ms obtained from Eqs. (3), respectively. In this case, the initial conditions should be that $w_{13}(0)=0$ and $G(0)=2$ as described in the Appendix. However, the curves thus plotted were not in agreement with the experiments. In order to obtain good agreement between the experiment in Fig. 6 and the theory, $G(0)$ was taken to be $2B$ with $B=0.40$, where it is also assumed that the DQ ADRF was incomplete. It is to be noted that the good agreements are seen not only in Fig. 6 but also in Fig. 7. The phenomenon in Fig. 7 is observed by using both the operations of AMRF and DQ ADRF. The theoretical curve in Fig. 7 is plotted with the same factors of A and B as those in Figs. 4 and 6, respectively. Therefore, the good agreement in Fig. 7 supports the above assumptions on the operations of AMRF and DQ ADRF.

IV. SUMMARY

The thermal mixing induced by the rf electric field between the two-level system with $\Delta m=\pm2$ and the dipolar system in the rotating frame has been investigated on ^{27}Al nuclei in Al_2O_3 in detail. The experiments were performed at room temperature using the slightly off resonant rf electric field with amplitude of 22.3 kV/cm. The thermal mixing is completely accomplished in a time much shorter than the spin-lattice relaxation time. The indirect saturations of the Al spins due to the defects of the lattice can be neglected under the strong rf electric field.

Two types of experiments were carried out. In the first one the rf electric field is applied to the spin system in thermal equilibrium at lattice temperature. In this case, the decreasing of the population difference w_{13} and the enhancement of the dipolar order are observed. In the second one, the DQ ADRF is performed before the rf electric field is applied to create the initial dipolar order in a high degree. In this case, w_{13} is produced as the dipolar order is destroyed. When the frequency offset $2\delta=\omega-(\omega_1+\omega_2)$ of the rf electric field is positive, the negative dipolar temperature and the negative population difference are produced by experiments I and II, respectively. These phenomena come from the fact that the energy of level 3 which is lower than that of level 1 in the laboratory frame becomes higher in the rotating frame.

The experimental results are well described by the exponential functions derived from the theory of the thermal mixing analogous to the Provotorov's theory. The excellent agreements between the experiments and the theory show that the concept of spin temperature in the rotating frame is valid when the strong rf electric field is used for the saturation, and the dipolar system represented by the Hamiltonian $\mathcal{H}_d^*$ which has so far been treated in NMR studies on the same spin system plays the role of the reservoir in the thermal mixing.

ACKNOWLEDGMENTS

I would like to thank Dr. H. Arakawa of Yokaichi Plant, Murata Mfg. Co., Ltd. for his sample processing using the epoxy powder. I am indebted to Professor T. Hashi for his critical reading of a draft manuscript and to Mr. K. Hayashi for his assistance in instrumentation.

APPENDIX

Under the experimental conditions described in Sec. II, the spin system of the Al spins is governed by the in-

dependent spins Hamiltonian

$$\mathcal{H}_0=-\omega_2 I_z+\omega_q[I_z^2-\tfrac{1}{3}I(I+1)]\ , \tag{A1}$$

where $\omega_q=\frac{1}{2}(\omega_1-\omega_2)$, and by the truncated dipolar spin-spin coupling Hamiltonian $\mathcal{H}_d^*$ which commutes with $\mathcal{H}_0$.

A static electric-field E applied along the x axis induces an additional electric-field gradient (efg) whose tensor elements are given with the R tensor as[18]

$$\begin{aligned} V'_0&=0\ ,\\ V'_{\pm1}&=(R_{113}\pm iR_{123})E\ ,\\ V'_{\pm2}&=(R_{111}\mp iR_{222})E\ . \end{aligned} \tag{A2}$$

A Hamiltonian $\mathcal{H}_p$ representing the electric quadrupole interaction with the induced efg is of a well-known form.[22] Using operators defined by[13,20]

$$\begin{aligned} Q_x(m,n)&=|m\rangle\langle n|+|n\rangle\langle m|\ ,\\ Q_y(m,n)&=-i(|m\rangle\langle n|-|n\rangle\langle m|)\ ,\\ Q_z(m,n)&=|m\rangle\langle m|-|n\rangle\langle n|\ , \end{aligned} \tag{A3}$$

spin operators I_+ and I_- in $\mathcal{H}_p$ are expressed by

$$I_\pm=\tfrac{1}{2}\sum_{m=-I+1}^{I}\alpha_m[Q_x(m,m-1)\pm iQ_y(m,m-1)]\ , \tag{A4}$$

where $|m\rangle$ and $|n\rangle$ are eigenfunctions of I_z, and

$$\alpha_m=\langle m|I_+|m-1\rangle\ . \tag{A5}$$

We assume that Eqs. (A2) also hold when $E=E_0\cos(\omega t)$. Then, $\mathcal{H}_p$ is given by

$$\begin{aligned} \mathcal{H}_p=(\omega_q/3V_{zz})E_0\cos\omega t\Big[&R_{113}\Big[\sum_m\alpha_m Q_x(m,m-1)I_z+I_z\sum_m\alpha_m Q_x(m,m-1)\Big]\\ &+R_{123}\Big[\sum_m\alpha_m Q_y(m,m-1)I_z+I_z\sum_m\alpha_m Q_y(m,m-1)\Big]\\ &+R_{111}\sum_m\alpha_{m+1}\alpha_m Q_x(m+1,m-1)-R_{222}\sum_m\alpha_{m+1}\alpha_m Q_y(m+1,m-1)\Big]\ , \end{aligned} \tag{A6}$$

where V_{zz} is an element of the internal static efg tensor.[22] In the following, the magnetic quantum numbers m and n in the operators in Eqs. (A3) are replaced by the corresponding numbers shown in Fig. 1 for convenience.

The time development of the spin system in the rotating frame under the irradiation of the rf electric field is described, in the interaction representation, by the equation of motion for the density matrix ρ of the spin system as

$$d\rho/dt=i[\rho,\delta Q_z(3,1)+\mathcal{H}_d^*+\mathcal{H}_p^*]\ , \tag{A7}$$

where effects of the spin-lattice relaxation are neglected, and

$$\mathcal{H}_p^*=U\mathcal{H}_pU^{-1} \tag{A8}$$

with a unitary operator

$$U=\exp[i\mathcal{H}_0t+i(-\delta t+\tfrac{1}{2}\phi)Q_z(3,1)]\ . \tag{A9}$$

The Hamiltonian $\mathcal{H}_p^*$ includes many fast-oscillating terms. Neglecting the fast-oscillating terms we can approximate as

$$\mathcal{H}_p^*=\tfrac{1}{2}\omega_pQ_x(3,1)\ , \tag{A10}$$

with

$$\omega_p=(\omega_q/3V_{zz})E_0\alpha_2\alpha_3(R_{111}^2+R_{222}^2)^{1/2}\ , \tag{A11}$$

where the phase angle ϕ in the operator U is given by

$$\exp(i\phi)=(R_{111}-iR_{222})/(R_{111}^2+R_{222}^2)^{1/2}\ . \tag{A12}$$

There are four kinds of Al sites (site a, b, c and f) in the crystal.[18] The phase ϕ is different in each kind of site because of the differences in signs of R_{111} and R_{222}.[18] Especially, the phases ϕ at sites a and b are 180° out of phase to those at sites f and c, respectively. Therefore, when DQ coherence is created by the EQ excitation, the macroscopic DQ coherence given from a superposition of the DQ coherences at all the sites will not be observed in contrast to the DQ coherence excited by the rf magnetic field.[8,9]

The theory of the thermal mixing is developed based on Eq. (A7) with Eq. (A10) in a manner similar to that of Provotorov.[4,5] In this case, the above-mentioned phase complication in the EQ excitation has no influence on the development of the theory because the treated density matrix is diagonal. We assign parameters $\beta(t)$ and $\zeta(t)$ including the inverse spin temperatures[4] to the Hamiltonians $\delta Q_z(3,1)$ and $\mathcal{H}_d^*$, respectively. Then, ρ is given, under the high-temperature approximation, by

$$\rho(t)=[1-\beta(t)\delta Q_z(3,1)-\zeta(t)\mathcal{H}_d^*]/z\ , \tag{A13}$$

where z is the partition function. With the assumption that the DQ free-decay in the transition $1\leftrightarrow3$ is Gaussian with decay time T_2, the theory leads to equations

$$\begin{aligned} d\beta/dt&=-K(\beta-\zeta)\ ,\\ d\zeta/dt&=-(\delta^2/D^2)d\beta/dt\ , \end{aligned} \tag{A14}$$

where K and D^2 are given by Eqs. (4) in the text with

$$K_0=\tfrac{1}{2}\sqrt{2\pi}\omega_p{}^2T_2\ . \tag{A15}$$

The derivation of kinetic equations such as Eqs. (A14) in-

volves some rough approximations, whereas the thermodynamic relations used in the rest of the paper are very well justified.

The population difference $w_{13}(t)$ is represented by[13]

$$w_{13}(t)=\mathrm{Tr}[\rho(t)Q_z(3,1)]$$
$$=-\delta\beta(t)\mathrm{Tr}[Q_z(3,1)^2]/z \ . \quad \text{(A16)}$$

Substituting the solution of Eqs. (A14) for $\beta(t)$ into Eq. (A16), we obtain Eq. (3a) in the text, where $G(0)$ is given from

$$G(t)=D\zeta(t)\mathrm{Tr}[Q_z(3,1)^2]/z$$
$$=2N(2I+1)^{N-1}D\zeta(t)/z \ , \quad \text{(A17)}$$

which indicates a degree of the dipolar order. Equation (3b) is obtained by substituting the solution of Eqs. (A14) for $\zeta(t)$ into Eq. (A17).

It is easily understood that the value of w_{13} represented in units of w_0 is equal to the magnitude $2S_1$ measured in units of S_0, because $S_1/S_0=w_{12}/w_0$ and $w_{13}=2w_{12}$.

It is shown that the value of G in units of w_0 is equal to the magnitude of S_2 measured in units of S_0 if the operation of AMRF is ideally performed. The magnitude S_2 directly indicates the magnitude of the transverse magnetization M produced along the rotating field H_1 of the pulse D from the dipolar order, which is represented (in units of $\hbar$) as

$$M=\tfrac{1}{2}\gamma\alpha_2\mathrm{Tr}[\rho' Q_x(2,1)] \ , \quad \text{(A18)}$$

with

$$\rho'=[1+\tfrac{1}{2}\eta\alpha_2\gamma H_1 Q_x(2,1)-\eta\mathcal{H}_d^*]/z \ , \quad \text{(A19)}$$

where η is a spin temperature parameter. Since the entropy of the spin system does not change in the adiabatic process, η is given[22] by

$$\eta=D\zeta/[(\tfrac{1}{2}\alpha_2\gamma H_1)^2+D^2]^{1/2} \ , \quad \text{(A20)}$$

which is approximated to

$$\eta=D\zeta/(\tfrac{1}{2}\alpha_2\gamma H_1) \quad \text{(A21)}$$

because the final intensity of H_1 is much larger than the local field. Substituting Eq. (A21) into Eq. (A18), we obtain $M=\frac{1}{2}\gamma\alpha_2 G$. On the other hand, the transverse magnetization M_0 produced in the transition $1\leftrightarrow 2$ by applying the 90° pulse to the spin system in thermal equilibrium at lattice temperature is expressed by $M_0=\frac{1}{2}\gamma\alpha_2 w_0$. Therefore, $M=M_0$, that is, $S_2=S_0$ if $G=w_0$. Thus, $S_2/S_0=G/w_0$. It is also shown by a similar approach that in experiment II, $G(0)=2w_0$ if the operation of DQ ADRF is ideal.

[1] A. G. Redfield, Phys. Rev. **98**, 1787 (1955); A. Abragam, *The Principles of Nuclear Magnetism* (Oxford University Press, New York, 1961).

[2] C. P. Slichter and W. C. Holton, Phys. Rev. **122**, 1701 (1961); M. Kunitomo, H. Hatanaka, and T. Hashi, Phys. Lett. **49A**, 135 (1974).

[3] S. R. Hartmann and E. L. Hahn, Phys. Rev. **128**, 2042 (1962); F. M. Lurie and C. P. Slichter, *ibid.* **133**, A1108 (1964).

[4] M. Goldman, *Spin Temperature and Nuclear Magnetic Resonance in Solids* (Oxford University Press, New York, 1970), and references therein.

[5] B. N. Provotorov, Zh. Eksp. Teor. Fiz. **41**, 1582 (1961) [Sov. Phys.—JETP **14**, 1126 (1962)].

[6] W. I. Goldburg, Phys. Rev. **122**, 831 (1961); **128**, 1554 (1962).

[7] H. Hatanaka (unpublished).

[8] H. Hatanaka and T. Hashi, J. Phys. Soc. Jpn. **39**, 1139 (1975).

[9] H. Hatanaka, T. Terao, and T. Hashi, J. Phys. Soc. Jpn. **39**, 835 (1975).

[10] T. Kushida and A. H. Silver, Phys. Rev. **130**, 1692 (1963).

[11] E. Brun, R. Hann, W. Pierce, and W. H. Tanttila, Phys. Rev. Lett. **8**, 365 (1962); E. Brun, R. J. Mahler, H. Mahon, and W. L. Pierce, Phys. Rev. **129**, 1965 (1963).

[12] See, for example, D. I. Bolef, *Physical Acoustics IV,* edited by W. P. Mason (Academic, New York, 1966).

[13] H. Hatanaka and T. Hashi, J. Phys. Soc. Jpn. **50**, 3629 (1981).

[14] V. L. Momashnya and V. A. Shutilov, Fiz. Tverd. Tela (Leningrad) **19**, 185 (1977) [Sov. Phys.—Solid State **19**, 106 (1977)].

[15] H. Hatanaka and T. Hashi, Phys. Lett. **67A**, 183 (1978).

[16] S. Vega and A. Pines, in XIXth Ampere Congress on Magnetic Resonance and Related Phenomena, Heidelberg, West Germany, 1976 (unpublished).

[17] A. G. Anderson and S. R. Hartmann, Phys. Rev. **128**, 2023 (1962).

[18] R. W. Dixon and N. Bloembergen, Phys. Rev. **135**, A1669 (1964).

[19] R. V. Saburova, V. A. Golenishchev-Kutuzov, N. A. Shamukov, and M. I. Pirozhkov, Fiz. Tverd. Tela (Leningrad) **11**, 2530 (1969) [Sov. Phys.—Solid State **11**, 2041 (1970)].

[20] H. Hatanaka and T. Hashi, Phys. Rev. **B27**, 4095 (1983).

[21] H. Hatanaka, H. Deguchi, and T. Hashi, J. Phys. Soc. Jpn. **54**, 374 (1985); H. Hatanaka, Phys. Lett. **112A**, 471 (1985); H. Hatanaka and N. Tabuchi, J. Phys. Soc. Jpn. **56**, 1323 (1987).

[22] See, for example, C. P. Slichter, *Principles of Magnetic Resonance* (Springer-Verlag, Berlin, 1978).